Modulation of excitatory synaptic coupling facilitates synchronization and complex dynamics in a nonlinear model of neuronal dynamics

Michael Breakspear, School of Physics and Brain Dynamics Centre, University of Sydney, Australia
John R. Terry, Department of Mathematics, University of Queensland, Australia
Karl J. Friston, Functional Imaging Laboratory, University College London, U.K.

Abstract:

We study complex dynamical synchronization in a nonlinear model of a neural system constituted by local networks of densely interconnected excitatory and inhibitory neurons. Neural dynamics are determined by voltage- and ligand-gated ion channels. Coupling between the local networks is introduced via sparse excitatory to excitatory connectivity. It is shown that with modulation of this long-range synaptic coupling, the system undergoes a transition from independent oscillations to stable chaotic synchronization. Between these states exists a 'weakly' stable state with epochs of synchronization and complex intermittent desynchronization. This may facilitate adaptive brain function by engendering a diverse repertoire of dynamics and contribute to the genesis of complexity in the EEG

1. Introduction:

The mechanisms and function of cooperative behavior in large-scale neuronal systems is currently an active area of research. Synchronous oscillations between neurons have been proposed as a mechanism for perceptual 'binding' through the coupling of distinct neuronal populations to form dynamic cell assemblies, each encoding various aspects of a perceived object (Singer 1995). Evidence of coherent oscillations has been demonstrated in neurophysiological data (Gray 1989) and computational models of the cortex (Lumer 1997). However, in much of this research, only linear measures of synergistic activity are employed. The nonlinear properties of excitable membranes motivates the study of nonlinear aspects of synchronicity in neural systems. In this paper, we study nonlinear interdependence in a model neural system consisting of an array of coupled small-scale

neural subsystems. Each subsystem is constituted by densely interconnected excitatory and inhibitory neurons. These are then coupled together through sparse long-range excitatory projections to form a larger ('mesoscopic') array. The dynamics within and between the subsystems derive from the properties of voltage-gated ion channels and competition at post-synaptic ligand-gated channels. We study the types and stability of nonlinear synchronization and consider the possible role of these behaviors in adaptive brain function.

2. Evolution Equations.

The approach adopted in this study is to consider the behavior of local ensembles of neurons, with dynamical variables and parameters taken as ensemble averages. The scale of each ensemble is taken as the extension of pyramidal cell dendritic arbors, approximately 100-300 μm, or the size of cortical columns. This approach is motivated by the fact that neurons within columns tend to share the same physiological properties, exhibit dense reciprocal interconnectivity, show strong dynamical correlations and are thought to comprise the brain's elementary functional modules (Kandel *et al.* 2000). The dynamical variables studied are the mean membrane potential of local pyramidal cells, *V*, and inhibitory interneurons, *Z*, and the average number of 'open' potassium ion channels, *W*. The evolution equations are adapted from a study of epileptic seizures in hippocampal slices (Larter *et al.* 1999) consisting of coupled differential equations, which in turn are derived from the model of Morris and Lecar (1981). The main focus is on the mean cell membrane potential of the pyramidal cells, governed by the conductance of sodium, potassium and calcium ion through voltage-gated channels, plus the passive conductance of 'leaky' ions. We begin with current flow across the pyramidal cell membrane;

$$\frac{dV}{dt} = -g_{Ca} m_{Ca} (V - V_{Ca}) - g_{na} m_{na} (V - V_{na}) - g_K W (V - V_K) - g_L (V - V_L), \qquad (1)$$

where g_{ion} is the maximum conductance of each population of ion species if all channels are open, m_{ion} is the fraction of channels open and V_{ion} is the Nernst potential for that ion

species. Each voltage gated channel acts as a switch which opens when the membrane potential passes above a given threshold, V_T. Averaging over a population of such channels and assuming a Gaussian distribution of V_T around a mean for each species, we obtain the sigmoid-shaped 'neural activation functions',

$$m_{ion} = 0.5\left\{1 + \tanh\left(\frac{V - V_T}{\delta_{ion}}\right)\right\}, \tag{2}$$

where δ_{ion} incorporates the variance of this distribution. The fraction of open potassium channels is slightly more complicated, being governed by W, with

$$\frac{dW}{dt} = \frac{\phi(m_k - W)}{\tau}, \tag{3}$$

where ϕ is a temperature scaling factor and τ is a 'relaxation' time constant. At the cell soma, the membrane potential triggers an action potential if it exceeds a threshold determined chiefly by the sodium channel threshold potential. Averaging this over the ensemble of neurons and assuming once again a Gaussian distribution, we obtain,

$$Q_V = 0.5 x Q_{V\max}\left\{1 + \tanh\left(\frac{V - V_T}{\delta_V}\right)\right\}, \tag{4}$$

$$Q_Z = 0.5 x Q_{Z\max}\left\{1 + \tanh\left(\frac{Z - Z_T}{\delta_Z}\right)\right\}, \tag{5}$$

where the Q_{max} are the maximum rates of firing of the excitatory and inhibitory neurons respectively. The firing of each of these cell populations feeds back onto the ensemble through synaptic coupling to open ligand-gated channels and raise or lower the membrane potential accordingly. In the case of excitatory-to-inhibitory and inhibitory-to-excitatory connections, this is modeled as additional inputs to the flow of ions across the membrane channel, weighted by functional synaptic factors, a_{ei} and a_{ie} respectively. In the case of excitatory to excitatory connections, the rate of firing Q_v is assumed to lead to

a proportional release of glutamate neurotransmitter across the synapse, onto two classes of ligand-gated ion channels. One class, embodying AMPA channels, open an additional population of sodium channels, hence increasing the net conductance of sodium flow. The second class, representing NMDA receptors, open an additional population of *voltage-gated* calcium channels. Hence this action increases the maximum conductance of voltage-gated calcium channels. Finally, 'nonspecific' subcortical excitation is added to both populations of neurons with amplitude I modulated by a random noise component of amplitude δ. Thus we obtain,

$$\frac{dV}{dt} = -(g_{Ca} + r_{NMDA} a_{ee} Q_V) m_{Ca} (V - V_{Ca}) - (g_{na} m_{na} + a_{ee} Q_V)(V - V_{na}) - g_K W (V - V_K) - g_L (V - V_L) + a_{ie} Q_Z + a_{ne} I_\delta, \quad (6)$$

$$\frac{dZ}{dt} = b(a_{ni} I_\delta + a_{ei} Q_V), \quad (7)$$

where r_{NMDA} incorporates the ratio of NMDA to AMPA receptors. Each of the set of equations, (2)-(7) govern the dynamics within each local cell assembly. Coupling between N nodes can be parsimoniously introduced as competitive agonist excitatory action at the same populations of NMDA and AMPA receptors. Representing each node with a superscript, this can be incorporated by modifying equation (6) to,

$$\frac{dV^i}{dt} = -\left(g_{Ca} + (1-C) r_{NMDA} a_{ee} Q(V^i) + C r_{NMDA} a_{ee} < Q(V^j) > \right) m_{Ca} (V^i - V_{Ca}) - g_K W (V^i - V_K) - g_L (V^i - V_L) - \left(g_{na} m_{na} + (1-C) a_{ee} Q(V^i) + C a_{ee} < Q(V^j) > \right)(V^i - V_{na}) + a_{ie} Q(Z^i) + a_{ne} I_\delta, \quad (8)$$

for $i,j=1,\ldots,N$. C parameterizes the strength of excitatory coupling between cortical columns. If $C=0$ the systems evolve independently. $C>0$ introduces interdependences between consecutive columns. $C=1$ corresponds to maximum coupling, with excitatory input from outside each column surpassing excitatory input from within each column.

I	0.3
a_{ee}	0.4
a_{ei}	0.1
a_{ie}	1
a_{ne}	1
a_{ni}	0.4
r_{NMDA}	0.2
δ	0.001

In the sections that follow, we set all physiologically measurable parameters (the maximum conductances, threshold potentials and Nernst potentials) to their accepted values (Larter *et al.* 1999). Other parameters, such as I and the functional synaptic strengths and maximum firing rates, were chosen to generate dynamically plausible behaviour, including limit cycle and aperiodic dynamics. To the extent that these equations represent a *model* of neural dynamics with significant membrane channel complexity incorporated but other simplifications required, we argue that such this is justified. To begin, we set N=2.

3. Transition to Chaotic Synchronization.

With the parameters set to the above values and with no intercolumn coupling (C=0), each of the systems exhibit aperiodic asynchronous oscillations, as shown In Fig. 1.

Fig. 1(a)

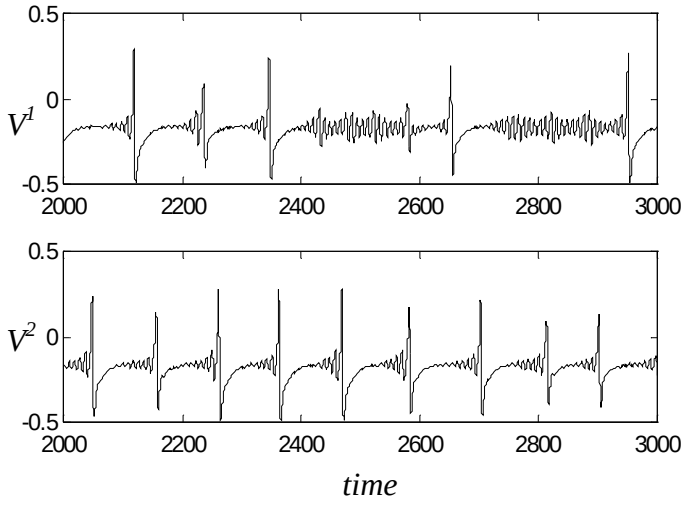

1(b)

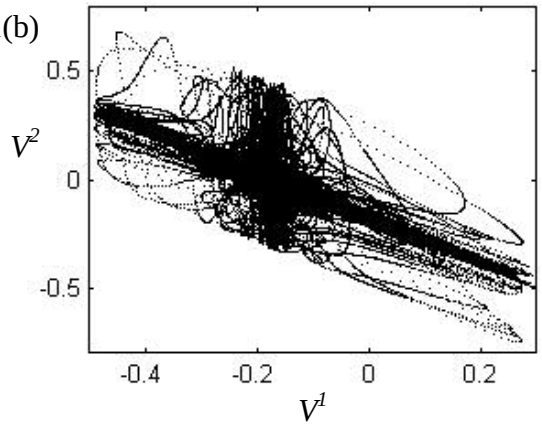

In Fig. 1(a) is shown a segment of the timeseries of each of the two subsystems, where it can be seen that the timeseries are aperiodic and asynchonous . In Fig. 1(b) we plot the concurrent values of V^1 and V^2 against each other, showing that they bear no close relationship. Using a Gram-Schmidt orthonormalization procedure, we find that the largest Lyaunov exponent for each system is approximately 0.02, indicative of chaotic motion. As expected, further exponents were identically zero and negative (-0.07).

With the introduction of coupling, $C>0$, the systems begin to show epochs of synchronized behavior. At $C\cong 0.2$, there is a transition to stable, fully synchronized

Fig. 2(a) 2(b)

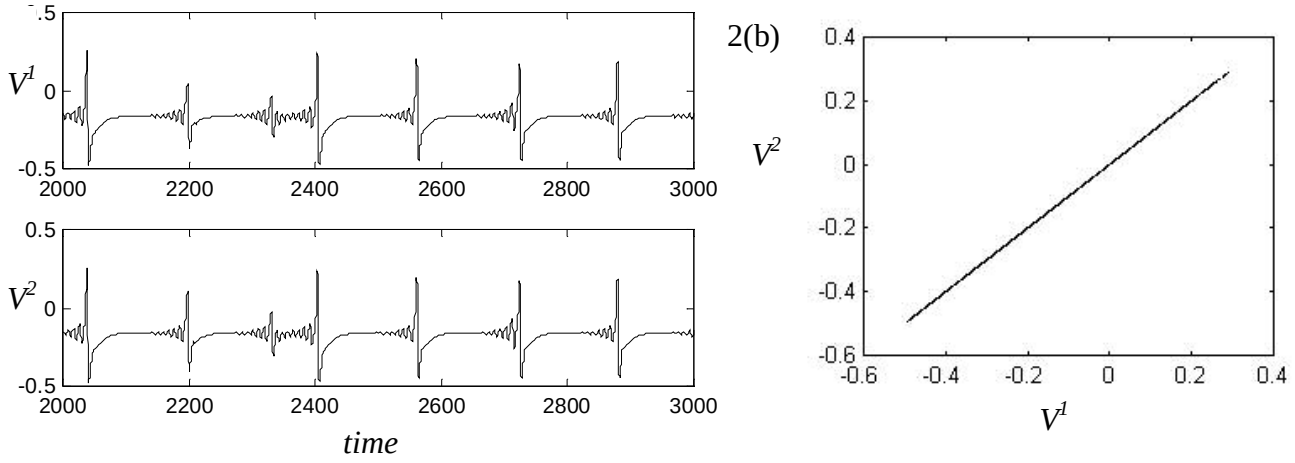

motion, as evident in the time series, Fig 2a. In Fig. 2(b) is presented the concurrent values of V^1 and V^2, illustrating that the system have become embedded in the low-dimensional 'symmetry manifold' $V^1 = V^2$. In addition to calculating the Lyapunov exponents for each system it is also possible to calculate the *transverse Lyaponuv exponents*, which describe the rate of separation of the coupled systems transverse to this manifold – in other words, the time-average tendency for the two systems to synchronize or separate.. For this strength of coupling, the largest transverse exponent is negative (-0.04), indicating that perturbations away from this state of identical synchronization decay, and thus that the state of identical chaotic synchronization is stable to noise. Whilst the phenomenon of chaotic synchronization has been widely studied since its initial description (Pecora *et al.* 1990), to our knowledge this is its first description in a detailed physiological model of coupled neural systems.

We note two other observations. Increasing r_{NMDA}, which corresponds to increasing the population of NMDA receptors, decreases the coupling strength required to achieve stable synchronization. On the other hand, increasing the overall excitatory-to-excitatory synaptic connectivity (a_{ee}) has the opposite effect. This is because the effect of local excitatory feedback, which tends to increase the local Lyapunov exponents, has the effect

of 'splitting' the synchronization and over-rides the opposing effect of increasing inter-columnar coupling.

4. Chaotic Phase Synchronization.

In the above simulations, all the parameters of both systems were equal. In real physiological systems, such symmetry between systems is clearly impossible. As a result, the symmetry manifold shown in Fig. 2b is not invariant under the action of the governing equations and hence *identical* synchronization between the coupled systems cannot be achieved. To incorporate this physiological variability, we introduced a random mismatch of between 0-10% for each of the physiological parameters.

Fig. 3(a)

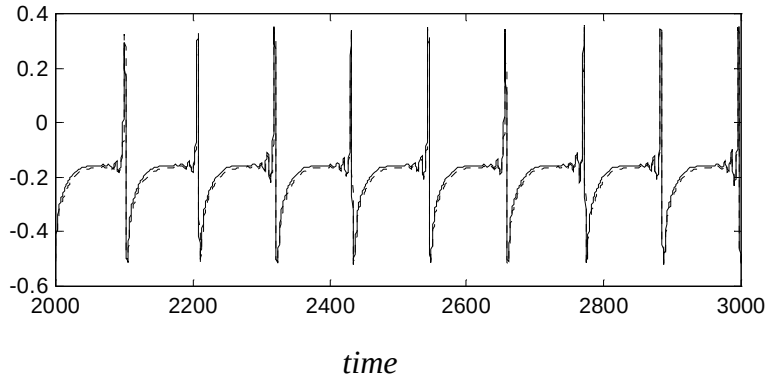

3(b)

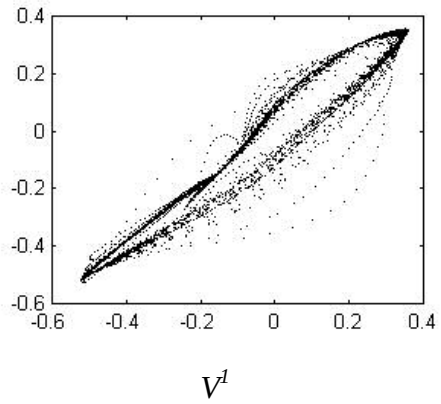

Fig. 3a shows the superimposed time series for an example simulation (V^2 dashed) with C=0.4. It can be seen that although the systems are not identical, strong phase synchronization is evident. In Fig. 3b, it is evident, that the attractor state for the coupled system has been 'pulled off' the symmetry manifold by the parameter asymmetries.

Fig. 4

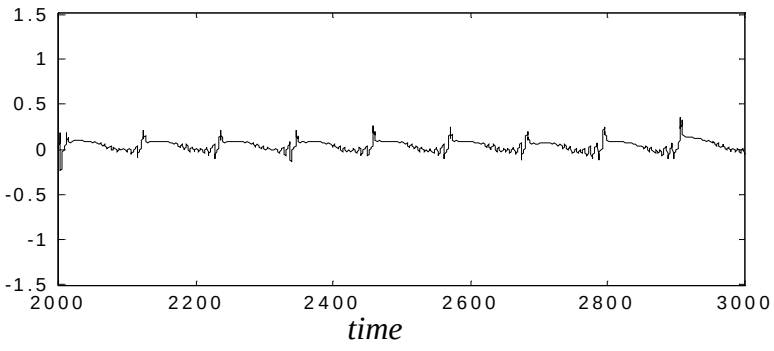

Phase synchronization can be made more evident if we use the Hilbert transform to extract the phase, ϕ of each signal (for further details, see Breakspear 2001). In Fig.

4 we plot the time series of the phase difference, $\varphi=\phi_1-\phi_2$ between the phases of V^1 and V^2 (for simplicity we plot sin(φ)). It can be seen that the phase difference is bounded (ie $|\phi_1-\phi_2|$<constant) which is the usual definition of phase synchronization.

5. Marginal Stability and Chaotic Transients.

When the coupling strength is set close to the threshold for stable chaotic synchronization (ie. The largest transverse Lyapunov exponents is approximately zero) one observes epochs of varying length interrupted by bursts of desynchronization. An example of such a phenomenon is given in Fig. 5. At *time*=600, it can be seen that the two time series briefly diverge from phase synchronization. This is evident in panel 5(b) as a brief violation of the criteria, $|\phi_1-\phi_2|$<constant).

Fig. 5a

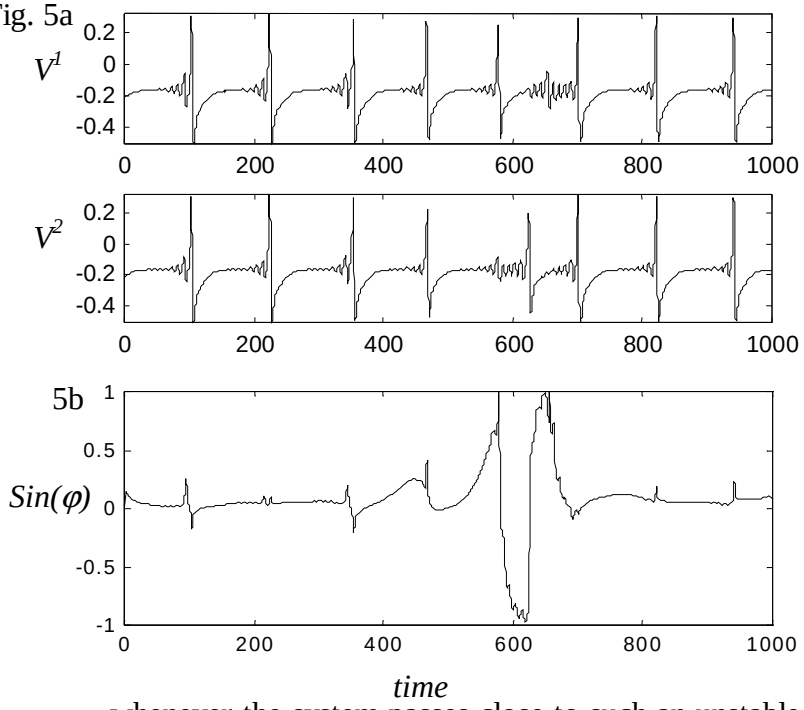

Such desynchronous bursts are known to be caused by *transversely unstable periodic orbits* embedded within the synchronized chaotic attractor. Desycnhronization occurs whenever the system passes close to such an unstable orbit (Heagy *et al.* 1988). We have previously argued (Breakspear 2001) that such 'marginal stability' may play a crucial role in normal brain function, permitting flexible and adaptive jumps between regional coherent states

In the brain, it may be unrealistic to create a rigid hierarchy between static state parameters and rapidly changing dynamic variables. Instead, it may be preferable to consider all parameters varying across a temporal hierarchy of several orders of

magnitude. For example, cell membrane potentials Z would be seen as occurring on a relatively fast scale. On the other hand the coupling parameter C and strength of effective excitatory connectivity a_{ee} are viewed as 'neuromodulatory' variables. These are set by slowly varying subcortical outputs, such as the activity within the monoaminergic system. Varying these parameters by only small amounts, in the system of equations (2)-(7), one sees switching between the variety of behaviors described above, each of which can be viewed as a complex and adaptive dynamical transient. It has been previously argued that such a dynamical landscape may optimize complex brain function (Friston 2001a, 2001b).

Analysis of larger arrays (N>2), with random variations in local parameters, reveals that at judicious coupling strengths, the array breaks up into separate synchronized clusters of various sizes. In addition, it is possible to 'induce' synchronization between selected subsystems by increasing the coupling strength between them. This allows an extra level of complexity to be introduced into the model. For example, it may allow targeted information transfer between a partial network of the entire array.

6. Discussion.

In this paper, we present a dynamical model for activity in an array of sparsely coupled local neural systems. The model incorporates the fundamental principles governing cell membrane potential as determined by voltage and ligand-gated ion channels. In this way, it allows a reasonable amount of physiological complexity to be incorporated, including synaptic activation and receptor subtypes. On the other hand, other neural properties, such as axonal and dendritic delays, are simplified. Numerical analysis of this model reveals a transition from independent oscillations to stable chaotic synchronization, depending on the balance of local versus long-range connectivity. These functional excitatory couplings are subject to subcortical neuromodulation. Chaotic phase synchronization occurs and is robust to system noise and random parameter variations.

Using an algorithm for the detection of nonlinear interdependence in experimental time series data (Schiff *et al.* 1997, Terry *et al.* 2002), it has recently been demonstrated that in scalp EEG recorded from healthy human subjects, nonlinear synchronization occasionally (<5% of epochs) overshadows linear correlations (Breakspear 2001, Breakspear *et al.* 2002). The nonlinear properties of these epochs closely resemble the behaviors discussed above. Further research is required to investigate the role of nonlinear interactions in large-scale brain dynamics.

References.

Breakspear, M. (2001) Nonlinear phase desynchronisation in human electroencephalographic data. *Human Brain Mapping* **15**: 175-198..

Breakspear, M., Terry, J. (2002) Detection and description of nonlinear interdependence in normal multichannel human EEG *Clin. Neurophysiol* (in press).

Friston, K. (2000a) The labile brain. I. Neuronal transients and nonlinear coupling. *Phil. Trans. R. Soc. Lond.* **355B**: 215-236.

Friston, K. (2000b) The labile brain. I. Transients, complexity and selection *Phil. Trans. R. Soc. Lond.* **355B**: 237-252..

Gray, C., Konig, P., Engel, A., Singer, W. (1989) Oscillatory responses in cat visual cortex exhibit inter-columnar synchronization which reflects global stimulus properties *Science* **338**: 334-337.

Heagy J, Carroll T, Pecora L, 1998. Desynchronization by periodic orbits, Phys Rev E 52: R1253-R1256.

Kandel, E., Schwartz, J., Jessell, T. (2000) Principles of Neural Science McGraw-Hill: New York.

Larter, R., Speelman, B. (1999) A coupled ordinary differential equation lattice model for the simulation of epileptic seizures *Chaos* **9**: 795-804.

Lumer, E., Edelman, G. Tononi, G. (1997) Neural dynamics in a model of the thalamocortical system. I. Layers, loops and the emergence of fast synchronous oscillations *Cerebral Cortex* **7**: 207-227.

Morris, C., Lecar, H. (1981) Voltage oscillations in the barnacle giant muscle fiber *Biophys. J.* **35**: 193-213.

Pecora L, Carroll T, 1990. Synchronization in chaotic systems *Phys Rev Lett* **64**: 821-824.

Schiff, S., So, P., Chang, T., Burke, R., Sauer, T. (1996) Detecting dynamical interdependence and generalized synchrony through mutual prediction in a neural ensemble. Phys. Rev. E **54**: 6708-6724.

Singer, W. (1995) Putative functions of temporal correlations in neocortical processing. In: Large-Scale Neuronal Theories of the Brain (Koch, C., Davis, J., eds) MIT Press: London.

Terry, J., Breakspear, M. (2001) An improved algorithm for the detection of nonlinear interdependence in bivariate timeseries data. (Submitted)